

Article

Cell Adhesion Strength Indicates the Antithrombogenicity of Poly(2-methoxyethyl acrylate) (PMEA): Potential Candidate for Artificial Small-Diameter Blood Vessel

Md Azizul Haque ^{1,2}, Daiki Murakami ^{1,3,*} and Masaru Tanaka ^{1,3,*}

¹ Department of Chemistry and Biochemistry, Graduate School of Engineering, Kyushu University, 744 Motooka, Nishi-ku, Fukuoka 819-0395, Japan; md.azizul.haque.509@kyushu-u.ac.jp

² Department of Applied Chemistry and Chemical Engineering, Noakhali Science and Technology University, Noakhali 3814, Bangladesh

³ Institute for Materials Chemistry and Engineering, Kyushu University, 744 Motooka, Nishi-ku, Fukuoka 819-0395, Japan

* Correspondence: daiki_murakami@ms.ifoc.kyushu-u.ac.jp (D.M.);

masaru_tanaka@ms.ifoc.kyushu-u.ac.jp (M.T.); Tel./Fax: +81-92-802-6238 (D.M. & M.T.)

Abstract: Poly(2-methoxyethyl acrylate) (PMEA) is a US FDA-approved biocompatible polymer, although there is insufficient work on human umbilical vein endothelial cells (HUVECs) and platelet interaction analysis on PMEA-analogous polymers. In this study, we extensively investigated HUVEC–polymer and platelet–polymer interaction behavior by measuring the adhesion strength using single-cell force spectroscopy. Furthermore, the hydration layer of the polymer interface was observed using frequency-modulation atomic force microscopy. We found that endothelial cells can attach and spread on the PMEA surface with strong adhesion strength compared to other analogous polymers. We found that the hydration layers on the PMEA-analogous polymers were closely related to their weak platelet adhesion behavior. Based on our results, it can be concluded that PMEA is a promising candidate for the construction of artificial small-diameter blood vessels owing to the presence of IW and a hydration layer on the interface.

Keywords: PMEA; HUVEC; platelet; interaction; hydration



Citation: Haque, M.A.; Murakami, D.; Tanaka, M. Cell Adhesion Strength Indicates the Antithrombogenicity of Poly(2-methoxyethyl acrylate) (PMEA): Potential Candidate for Artificial Small-Diameter Blood Vessel. *Surfaces* **2022**, *5*, 365–382. <https://doi.org/10.3390/surfaces5030027>

Academic Editor: Vladimir Lucian Ene

Received: 10 June 2022

Accepted: 25 July 2022

Published: 27 July 2022

Publisher's Note: MDPI stays neutral with regard to jurisdictional claims in published maps and institutional affiliations.



Copyright: © 2022 by the authors. Licensee MDPI, Basel, Switzerland. This article is an open access article distributed under the terms and conditions of the Creative Commons Attribution (CC BY) license (<https://creativecommons.org/licenses/by/4.0/>).

1. Introduction

In the modern era, owing to the unique properties of biocompatible polymers, they have been widely used in organ transplantation, tissue engineering scaffolds, development of medical devices, drug delivery systems, and biomedical healthcare sensors [1,2]. These biomaterials can be used in different ways, sometimes as a coating material or as an entire system made of the material itself to maintain the physiological and mechanical properties. Once biomaterials come in contact with the components of the living body, such as cells or proteins, they collaborate in distinctive ways. In particular, cells interact with the biomaterial interface through the extracellular matrix, which controls cell functions such as viability, growth rate, mobility, and protein secretion [3,4]. Therefore, cell adhesion study is one of the major concerns for biomaterials to become a perfect candidate for in vivo application in the human body. Consequently, cell adhesion capacity controls cell morphology, such as cell survival, proliferation, migration, and differentiation [5–7]. In contrast, platelet adhesion, as well as blood component adherence to the biopolymeric substrate, is also a vital phenomenon to become surface blood compatible [8].

Cardiovascular diseases (CVDs) are a threat to human health. Approximately 17.9 million people died of CVDs in 2019, which is 32% of the world's total deaths, and this number is expected to increase to 23.6 million by 2030 [9]. In CVDs, blood vessels are mostly blocked or narrowed by atherosclerosis or thrombosis. Atherogenesis is initiated by endothelial

dysfunction, and its movement leads to vessel damage and blocking, which causes thrombosis of the arterial wall as well as injury and dysfunction of tissues and organs [10,11]. Consequently, researchers are focusing on effective ways to reduce the causes of CVDs as well as the appropriate treatments of insured vessels, particularly for small-diameter blood vessels.

As an effective treatment, vascular graft transplantation with synthetic vascular grafts is an alternative option to replace injured vessels along with angioplasty, atherectomy, and stent insertion [12]. Currently, the available commercial artificial blood vessels are mostly made of polyethylene terephthalate (PET), polytetrafluoroethylene (PTFE), and dacron, which are used in large-diameter vessel transplants [13]. However, small-diameter vascular grafts are still under evaluation owing to thrombus formation inside the tube after implantation [14,15]. This implies that the interfaces of these synthetic polymers do not meet the requirements for transplantable grade or biocompatibility. Thus, the interfacial properties must be changed according to the compatibility state. Hence, an alternative method for changing the properties of the biopolymer interface is surface modification. Various surface modification techniques have been used to functionalize the interface of substrates for cell attachment, growth, migration, rapid endothelization, and long-term anticoagulation [9,16,17]. Polymer coating is an effective approach for functionalizing biomaterial surfaces. It is well established that functionalization with poly(ethylene glycol) and zwitterionic polymers, including poly(2-methacryloyloxyethyl phosphorylcholine) (PMPC), suppresses biofilm formation, immune responses to the biomaterial surfaces, and the adhesion of platelets [18–20]. Therefore, polymers with antifouling and antithrombogenic properties and strong endothelial cell attachment ability are desirable for scientists to obtain artificial small-diameter blood vessels (ASDBV).

Poly(2-methoxyethyl acrylate) (PMEA) is a FDA-approved biocompatible polymer that is used as an antithrombogenic coating polymer in several sophisticated medical devices such as artificial hearts and lungs, stents, catheters, and dialyzers [8,21]. A remarkable characteristic of PMEA is its unique interaction with water molecules, which play a dominant role in the biological environment and are detected using differential scanning calorimetry (DSC) [22], infrared spectroscopy [23], nuclear magnetic resonance [24], and several other approaches. Using DSC measurements, Tanaka et al. classified water molecules interacting with PMEA into three types: free water (FW), freezing-bound water (intermediate water; IW), and non-freezing water (NFW) [25]. IW plays an important role in surface biocompatibility. In a previous study, it was found that PMEA can reduce protein adsorption and platelet adhesion by suppressing the conformational change of fibrinogen [8,26]. Recently, it has been reported that non-blood cells can attach to the coated surface of PMEA and its analogues through integrin-dependent and integrin-independent mechanisms [27]. We also observed that integrin-independent cell attachment occurred on the PMEA-coated surface. Therefore, it is possible to find a suitable polymer that can be used to develop an implant biomaterial, such as an artificial blood vessel, if we can investigate human umbilical vein endothelial cells (HUVECs) and human platelet adhesion behavior (survival, proliferation, migration, differentiation, and interaction strength) on the surface of PMEA analogues.

HUVECs have been acknowledged as a useful model for research on the human endothelium [28]. HUVECs are an excellent model for the study of vascular endothelial properties and the main biological pathways involved in endothelial function, although this model does not represent all endothelial cell types found in an organism [29]. In contrast, the endothelium acts as a barrier between the blood and organs, and at the same time, is responsible for the transfer of nutrients, hormones, and white blood cells, as well as anti-inflammatory responses [30]. Moreover, blood pressure, flow, and coagulation are regulated by this organ [31]. In addition, HUVECs are also effective in studying hemodynamic interactions between the endothelium layer and atherosclerotic plaque formation because they allow exposure of endothelial cells (ECs) to shear stress controlling flow conditions, and therefore, represent blood flow conditions as in vivo [32]. Furthermore, ECs play a role

in angiogenesis and platelet binding to substrates and endothelial monolayers under flow conditions [33].

To develop a transplantable ASDBV (<6 mm), the construction materials should have the following properties: (1) biocompatibility to prevent an immune reaction against the artificial vessel, (2) cytophilic properties that enable endothelial and smooth muscle cells to migrate, and (3) properties that prevent thrombus formation [34]. To meet these requirements, it is important to investigate HUVECs integration into the construction polymer. In a previous study, Sato et al. reported the compatibility of PMEAs with the adhesion and proliferation of endothelial and smooth muscle cells [34]. Hoshiba et al. investigated the adhesion of the cancer cell line HT-1080, a fibrosarcoma cell line, on PMEAs analogues, with single-cell force microscopy [27]. HUVECs are the key cells in native blood vessels and have an important influence on the development of artificial blood vessels as the same confluent layer over the synthetic surface. However, there is no significant study on the interaction between the polymer surface and HUVECs by force measurement. In contrast, a recently published report described the design of a biocompatible elastomer using a PMAE–silica composite to obtain a tough and tube-like structure of ASDBV compared to the native vessel [35–37]. They reported that the mechanical properties of the PMAE–silica composites are comparable to those of native blood vessels and that the antithrombotic properties do not change with a slight increase in silica adhesion, although there is no evidence of endothelial cell adhesion ability.

In this study, the surface interaction of HUVECs on PMAE and its analogues was quantitatively investigated by force measurement for the development of ASDBVs. We also compared platelet adhesion behavior and time profiles of initial cell attachment. Furthermore, we observed the hydration states of the polymer interfaces using frequency-modulation atomic force microscopy (FM-AFM). Finally, we related the results of single-cell force spectroscopy (SCFS) and FM-AFM to characterize HUVECs attachment and platelet adhesion mechanisms on PMAE-analogous surfaces.

2. Materials and Methods

2.1. Chemicals and Materials

Polyethylene terephthalate (PET) was purchased from Mitsubishi Plastic Inc. (Tokyo, Japan). Poly(2-methoxyethyl acrylate) (PMAE, $M_n = 26.9$ kg/mol, $M_w/M_n = 2.73$), poly(3-methoxypropyl acrylate) (PMC3A, $M_n = 20.8$ kg/mol, $M_w/M_n = 3.83$), and poly(*n*-butyl acrylate) (PBA, $M_n = 62.8$ kg/mol, $M_w/M_n = 1.41$) were synthesized according to a previous report [38]. Poly(*n*-butyl methacrylate₇₀-co-2-methacryloyloxyethyl phosphorylcholine₃₀) (PMPC, $M_w = 600$ kg/mol) was donated by the NOF Corporation, Japan. Tissue culture polystyrene (TCPS) was purchased from IWAKI, Shizuoka, Japan. Fibronectin was obtained from Wako Pure Chemical Industries (Osaka, Japan). Human whole blood for the platelet adhesion test was purchased from Tennessee Blood Services (Memphis, TN, USA) and collected in a vacuum blood collection tube (Venoject II, Terumo Co., Tokyo, Japan) containing 3.2% sodium citrate as an anticoagulant. Human whole blood was collected within a week of blood collection. Blocking reagent was purchased from Nacalai Tesque (Kyoto, Japan). All other reagents and solvents were obtained from Kanto Chemical Co. (Tokyo, Japan).

2.2. Fabrication of Polymer-Coated Substrates

PET was used as a substrate for coating. One side of the PET sheet (thickness = 120 μm) was indicated as the coating side. Prior to coating, the PET sheet was cut into a circle with a diameter of 14 mm. Each PET substrate was dipped in toluene 2–3 times and then dried in air. PMAE, PMC3A, and PBA were dissolved in Toluene (0.5 $w/v\%$) to make a polymer solution. PMPC was dissolved in methanol at the same concentration. PMAE analogue polymer solutions (26.2 $\mu\text{L}/\text{cm}^2$) were spin-coated on the PET substrates using a Mikasa Spin Coater MS-A100 (Mikasa Co., Ltd, Tokyo, Japan) at a constant rate of 3000 rpm for 40 s, ramped down for 4 s, and thereafter dried for at least 24 h in a vacuum dryer at

25 °C. The stability of prepared films was confirmed by the contact angle measurement after immersion in water.

2.3. Contact Angle (CA)

CA represents the wettability of studied polymers. CA measurements were performed using Milli-Q water. The CA values of PMEA-analogous surfaces were calculated using two methods: (1) sessile drop of water and (2) air bubble in water at 25 °C using a DropMaster DMO-501SA (Kyowa Interface Science Co., Tokyo, Japan). In the sessile drop method, a 2 µL water droplet was placed on the polymer surface for 60 s, and the CAs were measured using photographic images. The droplet method was executed by placing 2 µL of water droplets on the five positions of each substrate. We conducted the measurement three times with three different substrates. So, the total number of images was 15 for the droplet method. In the captive bubble method, PMEA-analogous substrates were immersed in Milli-Q water for 24 h. Thereafter, 2 µL of air bubbles were injected beneath the substrate surfaces located in water, and the CAs were measured using photographic images. Finally, the CA at 30 s was counted as the CA of the substrate.

2.4. Cell Culture

Endothelial cells were used for all experiments described in this article. Commercially available human umbilical vein endothelial cells (HUVECs) (Lonza, Cologne, Germany) were cultured under static cell culture conditions (37 °C, 5 vol% CO₂) in polystyrene-based cell culture flasks. Cells were used for 4 to 6 passages and cultured in endothelial basal medium (EBM-2) supplemented with endothelial growth medium (EGM-2), Single Quots[®] kit, and 2 vol% FCS (Lonza, Cologne, Germany). Prior to the experiments, cells were detached from the culture dish using 0.25% trypsin/EDTA solution (Thermo Fisher Scientific, Rockford, IL, USA). The HUVECs solution was centrifuged at 1200 rpm for 3 min to isolate HUVECs from the old medium. Initial cell counting was performed using a hemocytometer to adjust the cell density.

2.5. Cell Attachment and Proliferation Assay

Cell attachment and proliferation assays were performed using a 24-well plate (IWAKI, Tokyo, Japan). Initially, the 24-well plate was coated with PMPC (0.5 w/v%) and stored for drying. The precoated polymer substrates were thereafter fixed in the 24-well plate using glue on the back side of each substrate. The substrates were then cured under ultraviolet (UV) light for 30 min. Phosphate-buffered saline (PBS) was then added to the well and stored in the incubator for 1 h at 37 °C. Afterwards, PBS was removed, and culture media were added and incubated under the same conditions for another 1 h at 37 °C. HUVECs were seeded on the substrates at 1×10^4 cells/cm² in serum-containing media and allowed to adhere and proliferate on the surface of the substrates for 1 d, 3 d, 5 d, and 7 d. The culture media were changed every two days for 3 d, 5 d, and 7 d. After cell cultivation, at specific time intervals, the cells were counted using a microplate analyzer from the standard curve prepared by the colorimetric WST-8 assay (Dojindo Laboratories, Kumamoto, Japan).

2.6. Immunocytochemical Analysis

Before starting the experiment, the prepared substrates were preconditioned, as in the cell attachment and proliferation assays. HUVECs (5×10^3 cells/cm²) were thereafter seeded on each polymer-coated substrate ($\varphi = 14$ mm) and incubated for 1, 24, and 72 h. After culturing for specific times, the cells were fixed using preheated (37 °C) 4% (w/v) paraformaldehyde (Fujifilm Wako Pure Chemical Corporation, Osaka, Japan) and stored outside for 10 min. Thereafter, 1% (v/v) Triton X-100 (Fujifilm Wako Pure Chemicals Co., Ltd., Osaka, Japan) in PBS (–) was added to increase plasma membrane permeability. After washing, the sections were blocked for 30 min. The substrates were thereafter treated with mouse monoclonal anti-human vinculin antibody (VIN-11-5; Sigma-Aldrich, St. Louis, MO, USA)(1:200) diluted in PBS (–) for 90 min at room temperature, and subsequently treated

with Alexa Fluor 568-conjugated anti-mouse IgG (H + L) antibody(1:1000 dilution), Alexa Fluor 488-conjugated phalloidin (1:1000 diluted), DAPI (4,6-diamidino-2-phenylindole (1:1000 diluted)) (all from Thermo Fisher Scientific, Waltham, MA, USA), and all diluted in 10% blocking solution in PBS, treated for 1 h at room temperature. After performing these steps, stained cells were fixed on glass slides. Fluorescence images were captured using a confocal laser scanning microscope (CLSM) (FV-3000; Olympus, Tokyo, Japan).

2.7. HUVECs–Polymer Interaction by SCFS

The PMEA-analogous substrates were exposed under UV for 30 min and thereafter incubated with PBS for 1 h at 37 °C. Subsequently, an EGM-2 medium was added to the substrate and freshly detached cells (passage: 5–6) were injected. In contrast, the tipless cantilever TL-CONT (spring constant $k = 0.2 \text{ N/m}$, NANOSENSORS) was coated by fibronectin with human fibronectin solution (1 mg/mL) for 20 min at room temperature. A single HUVEC was captured with a tipless cantilever for 10 min of holding time (set point: 2 nN) (Figure S1 in Supplementary Materials). The Z-length for a cell was 100 μm of the vertical displacement range of the AFM. We have found that the HUVEC cells are around 20 μm in size. A cell detached at about 70–90 μm . The force curves between the cell and the substrate were recorded using an atomic force microscope AFM (CellHesion, Bruker, Billerica, MA, USA) equipped with a cell-attached tipless cantilever (set point: 2 nN, approach rate: 5.0 $\mu\text{m/s}$, holding time: 120 s, retraction time: 15 $\mu\text{m/s}$) (Figure S3). A single cell was used to measure 1–3 interactions to avoid the effect of damage of cell on measurement. The measurements were conducted at more than 10 different points. The set point for measuring the cell adhesion strength was determined from the relationship between the set points and the cell adhesion strength of HUVECs attached to the PMEA-coated PET substrate [39]. In brief, we selected contact time 120 s and set point 2 nN after investigating different contact times (60, 120, 240, and 300 s) at different set points (0.5, 1, 2, 3, and 5 nN). Linear relationships between contact time and adhesion force and set point and adhesion force were found. As we know, HUVECs are very slow with doubling time (24–36 h). So, we fixed contact time 120 s because initial contact would not happen earlier due to slow doubling time. In contrast, we realized that at fixed set point 2 nN and 120 s contact time, HUVECs showed considerable adhesion force. The adhesion force was defined as the maximum force for the detachment of the cell from the substrate, corresponding to the force at the minimum point of the retraction curve. Adhesion work was estimated as the amount of work required to detach the cell from the substrate, corresponding to the area enclosed by the baseline and retraction curve [40].

2.8. Human Platelet Adhesion Test

The antithrombotic properties of the hybrids were evaluated using the human platelet adhesion test. Human platelet adhesion tests were performed according to our previously reported procedure [41]. In brief, human whole blood was centrifuged at $400 \times g$ for 5 min to collect platelet-rich plasma (PRP). The residue was also centrifuged at $2500 \times g$ for 10 min to collect platelet-poor plasma (PPP). Plasma solution containing platelets was prepared by adjusting the seeding density to $4 \times 10^7 \text{ cells/cm}^2$ by mixing PRP and PPP obtained from fresh human whole blood. The plasma solution (200 μL) was placed on each polymer substrate cut into $8 \times 8 \text{ mm}$ squares, and the substrates were incubated at 37 °C for 1 h. After 1 h of incubation, each substrate was rinsed with PBS (–), and then the platelets adhered to the substrates were fixed by immersing in 1% glutaraldehyde in PBS(–) for 2 h at 37 °C. Finally, each substrate was rinsed with PBS(–) and pure water and then dried. The number of adhered platelets was counted by scanning electron microscopy (SEM).

2.9. Platelet–Polymer Substrate Interaction by SCFS

Prior to this experiment, PMEA-analogous substrates were exposed under UV for 30 min and thereafter incubated with PBS for 1 h at 37 °C. The supplied fresh blood was centrifuged at $400 \times g$ for 5 min to obtain platelet-rich plasma (PRP), and the remaining

blood was centrifuged at $2500 \times g$ for 10 min to obtain platelet-poor plasma (PPP). PPP was thereafter added to the substrate, and freshly collected platelets (PRP-10 μL) were injected into the PPP. Meanwhile, the tipless cantilever TL-CONT (spring constant $k = 0.2 \text{ N/m}$, NANOSENSORS) was treated with human fibronectin solution (1 mg/mL) for 10 min. A single platelet was captured with a tipless cantilever for holding time of 5 min (set point: 2 nN) (Figure S2). The Z-lengths for platelets were 50 μm to ensure a complete separation of cells. The average size of the platelets was 1.5–3 μm and they detached at about 7–10 μm . The force curves between the platelets and the substrates were recorded using an AFM (CellHesion, JPK) equipped with a platelet-attached tipless cantilever (set point: 2 nN, approach rate: 1.0 $\mu\text{m/s}$, holding time: 10 s, retraction time: 5 $\mu\text{m/s}$) (Figure S4). The measurements were conducted at more than 5 different points.

2.10. FM-AFM of Single HUVEC Surface

FM-AFM was performed using a SPM-8100FM (Shimadzu Co., Kyoto, Japan) in water at 23 °C. A PPP-NCHAuD cantilever (typical spring constant, $k = 42 \text{ N/m}$, NanoWorld AG) was used. The resonance frequency in water was approximately 140 kHz, and the z-direction scan was performed with a force limit of 2 V, which corresponded to a frequency shift of ca. 400 Hz. The amplitude of the cantilever oscillation was maintained constant at approximately 2 nm.

2.11. Statistical Analyses

Data are expressed as mean \pm standard deviation (SD) of at least three independent trials. The significance of the differences between the means of the individual groups was assessed by one-way analysis of variance followed by the Tukey–Kramer multiple comparison test using Origin Pro ver. 2019b (Northampton, MA, USA). Statistical significance was set at $p < 0.05$. Curve fitting was performed using the Origin Pro ver. 2019b (Northampton, MA, USA).

3. Results and Discussion

3.1. Physicochemical Properties of PME A-Analogue-Coated Surface

Figure 1 shows the chemical structures of the polymers investigated. Previously, it was clearly demonstrated that PME A-analogous polymers (PME A, PMC3A, and PBA) contained three different types of water: FW, IW, and NFW [41–44]. Based on this analysis, the physicochemical properties, including molecular weight (M_n), glass transition temperature (T_g), amounts of FW, IW, NFW, and equilibrium water content (EWC), are summarized in (Table 1). The amounts of each water content (FW, IW, NFW, and EWC) and T_g changed in the following order: PBA < PMC3A < PME A and PME A > PMC3A > PBA, respectively. It was also reported that the hydrophilicity of the side chain of a polymer was linked to hydrated water and cell attachment behavior [45]. In contrast, the surface morphologies of PME A-analogue-coated PET substrates were investigated using transmission electron microscope (TEM) and AFM previously. TEM observations indicated that the thickness of the spin-coated film was approximately 70–80 nm [46], and AFM topographic analysis identified the microphase-separated structure as polymer- and water-rich domains of specific coated substrates [47] in which the water-rich domain worked to reduce the adsorption of fibrinogen on PME A. In addition, because of the strong effect of the physicochemical properties of the biopolymer interface, the surface type was confirmed by CA measurements in dry and hydrated states. The CA of each coated substrate was measured using both sessile drop and captive air bubble methods (Table 2). The results were recorded for 60 s and presented herein at exactly 30 s. In the sessile drop measurements, the CA decreased in the following sequence: PMPC > PBA > PET > PMC3A > PME A, whereas results from captive air bubbles exhibited different trends as PMPC > PME A > PMC3A > PBA > PET at 30 s and 24 h of soaking. These results revealed that proper coating of each polymer on the PET substrate and hydration caused a structural change in the coated surface for specific coated substrates. No significant changes were observed for the PET substrates.

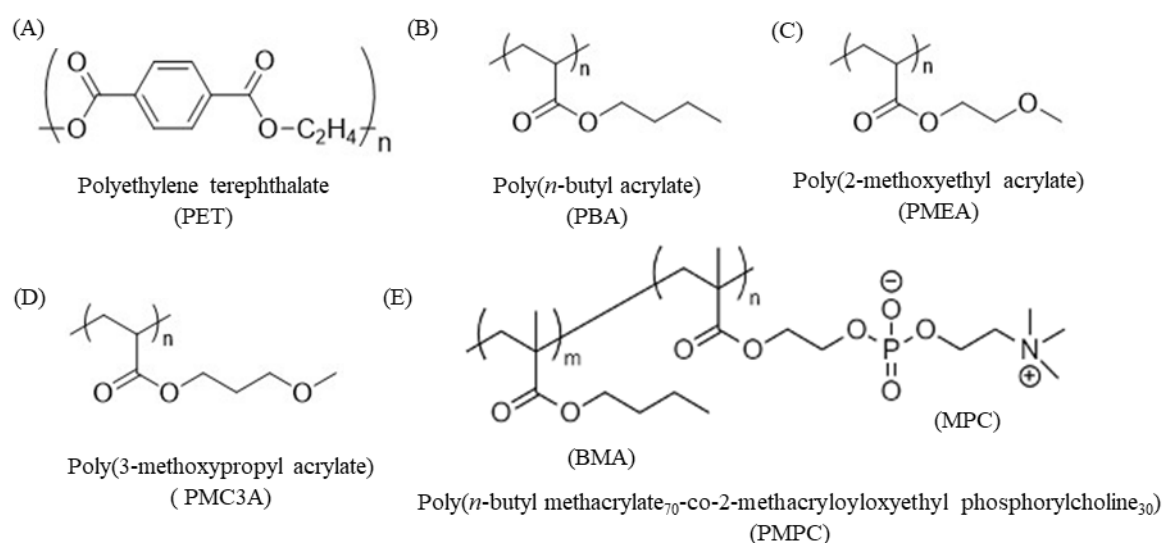


Figure 1. Chemical structure of (A) polyethylene terephthalate (PET); (B) poly(*n*-butyl acrylate) (PBA); (C) poly(2-methoxyethyl acrylate) (PMEA); (D) poly(3-methoxypropyl acrylate) (PMC3A), and (E) poly(*n*-butyl methacrylate₇₀-co-2-methacryloyloxyethyl phosphorylcholine₃₀) (PMPC).

Table 1. Characterization of PMEAs-analogous polymers.

Polymers	M_n	M_w/M_n	T_g Dry ^a	T_g Wet ^a	IW ^{a,b}	NFW ^{a,b}	FW ^c	EWC ^d
	(kg/mol)		(°C)	(°C)				
PBA	62.8	1.41	−47	−48	0.31	0.45	0.54	1.3
PMEA	26.9	2.73	−35	−51	3.7	2.5	2.5	8.7
PMC3A	20.8	3.83	−48	−58	2.8	3.1	1.7	7.6
PMPC	-	-	-	-	11.11	33.33	-	-

^a Measured by DSC performed at a rate of 5 °C/min, ^b intermediate water (IW) and non-freezing water (NFW) measured by DSC analysis, ^c free water (FW), and ^d equilibrium water content (EWC).

Table 2. CAs on the polymer surface*.

Polymers	CA [deg]		
	Sessile Water Drops	Captive Air Bubble	
	(30 s)	(30 s)	24 h
PET	73.3 (±0.9)	125.5 (±2.2)	125.4 (±0.5)
PBA	83.8 (±1.9)	126.7 (±2.8)	125.0 (±1.7)
PMEA	44.3 (±2.1)	134.0 (±0.9)	132.9 (±1.8)
PMC3A	52.1 (±0.5)	126.9 (±1.0)	127.8 (±0.7)
PMPC	108.9 (±0.5)	152.4 (±2.9)	150.0 (±3.8)

* 2 µL water droplet in air (sessile drop) and 2 µL air bubble in water (captive bubble). The data represent the means ± SD (*n* = 5).

3.2. Cell Attachment and Proliferation Assay

Toward the design of biomaterials, particularly ASDBs, the abilities of attachment, sustainability, and proliferation of endothelial cells on the coated substrate are some of the significant factors. From the anatomy of native blood vessels, it is known that blood vessels consist of three distinct layers: tunica externa or adventitia, tunica media, and tunica intima, which is the most inner layer [48]. Therefore, the endothelial cells are attached to this inner part, where blood is directly in contact with these cells and blood flows over there. Consequently, endothelial cells play a vital role in blood vessel compatibility. In this regard, we performed cell attachment and proliferation assays of HUVECs and attached cell morphology to evaluate whether the coated surface was viable, as shown in

Figure 2a,b. Initially, we seeded HUVECs on the substrate and evaluated the number of cells attached and proliferated after 1, 3, 5, and 7 days of culture. Thereafter, we observed that after 24 h of culture time, more than 50% of the seeding density (5×10^3 cells/cm²) of HUVECs adhered to PMEA, PBA, and PET. It indicates that the number of adhered cells on these polymers were almost similar to each other. In contrast, PMC3A showed comparatively lower numbers of HUVECs adhered on its surfaces, which was 42% of its seeding density. In contrast, PMPC and TCPS exhibited very low and high (127%) cell attachments, respectively, of negative and positive controls. As the culture time increased, on days 3 to 5 HUVECs proliferated gradually on PMEA, PBA, and PET. However, almost all cells had died on PMPC owing to lack of adherence, and the number of cells increased on TCPS, similar to the trend observed in previous studies. However, HUVECs numbers were increased more than two- and three-fold on PMEA, PMC3A, and PET, respectively, whereas PBA exhibited low amplification. The number of HUVECs on the substrates at day 7 decreased in the following order: TCPS > PET > PMEA > PMC3A > PBA > PMPC. However, the differences among PMEA, PMC3A, and PBA were not significant, even on day 7. Therefore, we performed further investigations using SCFS as a more quantitative and short-time investigation.

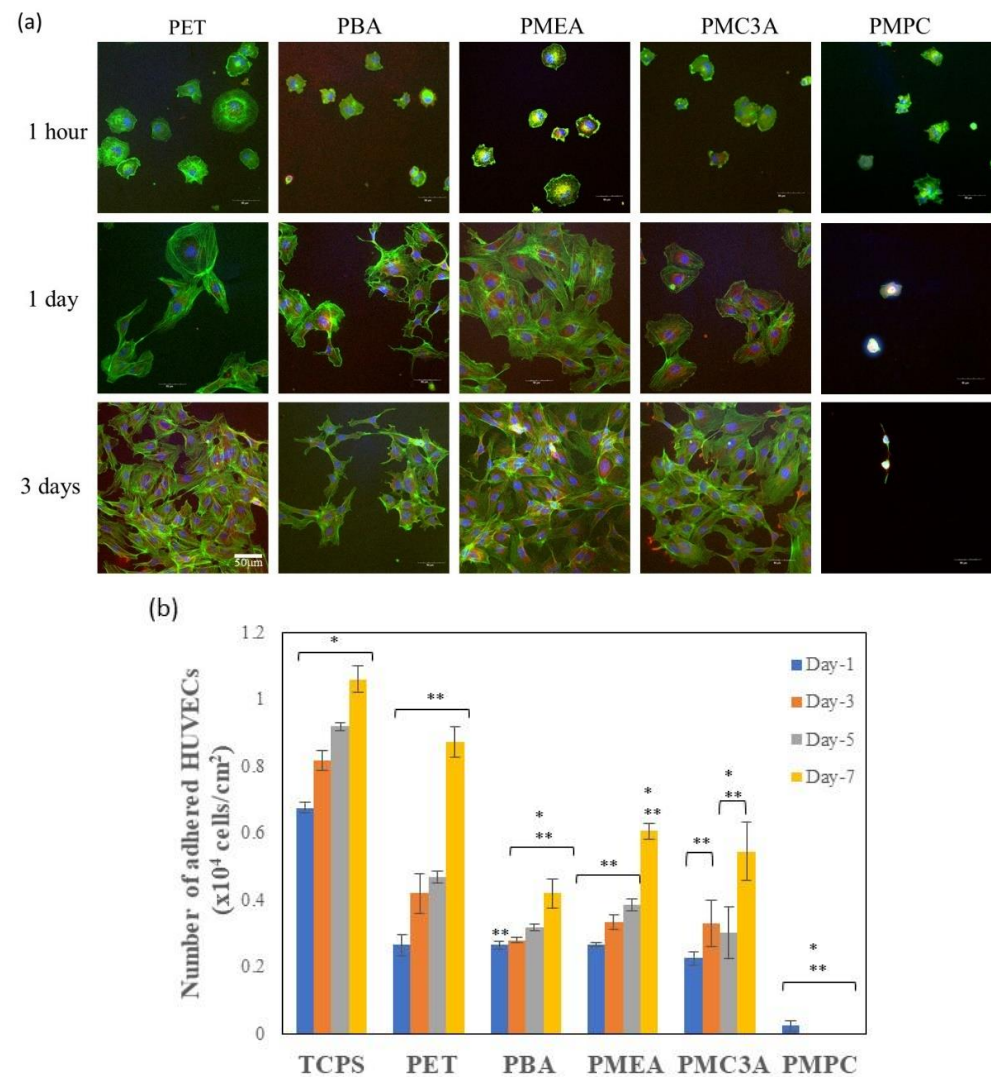


Figure 2. (a) CLSM images of PMEA-analogue-coated substrates. Blue: cell nuclei; green: vinculin; red: actin fibers. White bar indicates 50 μ m. (b) Numbers of adhered HUVECs on PMEA-analogue-coated substrates at 1, 3, 5, and 7 d. The data represent the mean \pm SD ($n = 3$), ** $p < 0.05$ compared with TCPS and * $p < 0.05$ compared with PET.

3.3. Measurement of Cell–Substrate Interaction Behavior by SCFS

One of the vital features before the construction of ASDBV is to obtain knowledge of the degree of adhesion strength of cell–substrate interactions at the interface of the synthetic polymers. When the blood flows inside the blood vessel, particularly over the layer of endothelial cells, it creates a certain shear force that can wash out the cells from the substrate surface if the adhesion strength is not sufficiently strong. Moreover, different cells have different interaction behaviors for specific surfaces, which may be strong or weak. In addition, cell types and surface characteristics are responsible for this phenomenon. Furthermore, surface modification with the investigation of substrate surface morphology such as roughness, hydrophilicity, hydrophobicity, and bound water content influences the cell adhesion strength [39]. Protein adsorption on the substrates also regulates the cell adhesion ability [49]. There is another possibility of tuning cell adhesion by chemical functionalization as in the case of neural cells where adhesion/repulsion has been controlled after suitable functionalization of metal electrodes [50]. Thus, quantitative investigation and comparison are required for the fabrication of an appropriate ASDBV. In this study, we evaluated the interaction strength between the cell membrane and PMEA-analogous substrates using SCFS. The SCFS measurement, which uses a single cell as a probe for the AFM cantilever, provides insights into the magnitude of the initial interaction force of a single cell in contact with the substrates [40]. In brief, AFM observation is considered as a multipurpose technique including imaging and detection of tiny interaction forces in a few pN levels between two surfaces. The SCFS mode of AFM technique may detect the interaction between single living cells and substrate or single cell, one is on the substrate, and the other one is adhered on the cantilever with the help of cell-adhering protein coating [51].

An animation is presented in Figure 3a to illustrate how cell–substrate interaction was measured and Figure 3b presents a force–distance (F-D) curve recorded with the CellHesion AFM technique. In brief, the cantilever was coated with fibronectin, and a single cell was captured and approached the measured substrate. Here, an interaction occurred between these two surfaces. After a while, the cantilever was retracted, and the data were represented as the force–distance curve (Figure 3b). The SCFS results are shown in Figure 4. We found that HUVECs adhered to PMEA more strongly than to other analogues. The adhesion strength and energy were similar to those of TCPS and PET. In contrast, PBA exhibited a low adhesion strength and energy for HUVECs adhesion. The adhesion on PMC3A was lower, but larger than that on PMPC.

Generally, cells adhere to the polymeric interface through cell-binding proteins. In serum-containing media, fibronectin, a cell adhesion protein, is responsible for cell adhesion through integrin, which is known as integrin-dependent cell adhesion [52]. However, it has been reported that integrin-independent cell adhesion may occur on PMEA through direct interactions between the cell membrane and the polymer surface [27]. In this case, protein adsorption on the PMEA surface was inhibited because of the presence of a hydration layer, where IW portion is the key factor. In our previous study, we observed that cells could adhere to the PMEA surface without FBS proteins [26,27]. Endothelial cells, such as HUVECs, are more likely to adhere to fibronectin than fibrinogen through the RGD sequence, which is known as a universal binding site [53–55]. In our study, PMEA-analogous polymers exhibited different adherences to HUVECs because of its surface characteristics and morphology. At hydrated condition, the PMEA-analogous polymers showed microphase separation and the protein adsorption behavior was different for each phase of each polymer. We are saying that protein adsorption regulates cell adhesion and we tried to find out how strong the cell adhesion was on each substrate by applying SCFS. From our previous investigations, more fibronectin adhered on water-rich domains whereas fibronectin and fibrinogen adsorption were similar on polymer-rich regions [49]. Fibronectin is responsible for cell adhesion and fibrinogen enhances the platelet adhesion. Furthermore, it is reported that PMEA contains 3.7% IW, whereas PMC3A and hydrated PBA contain 2.8 wt% and 0.31 wt% IW, respectively. It was also reported that more than 3 wt% IW is required to

give the surface better hemocompatibility for poly(ethylene glycol), poly(meth)acrylates, aliphatic carbonyls, and poly(lactic-co-glycolic acid) surfaces [56]. Therefore, owing to the different IW content, the cell adhesion number varied in our tested polymers.

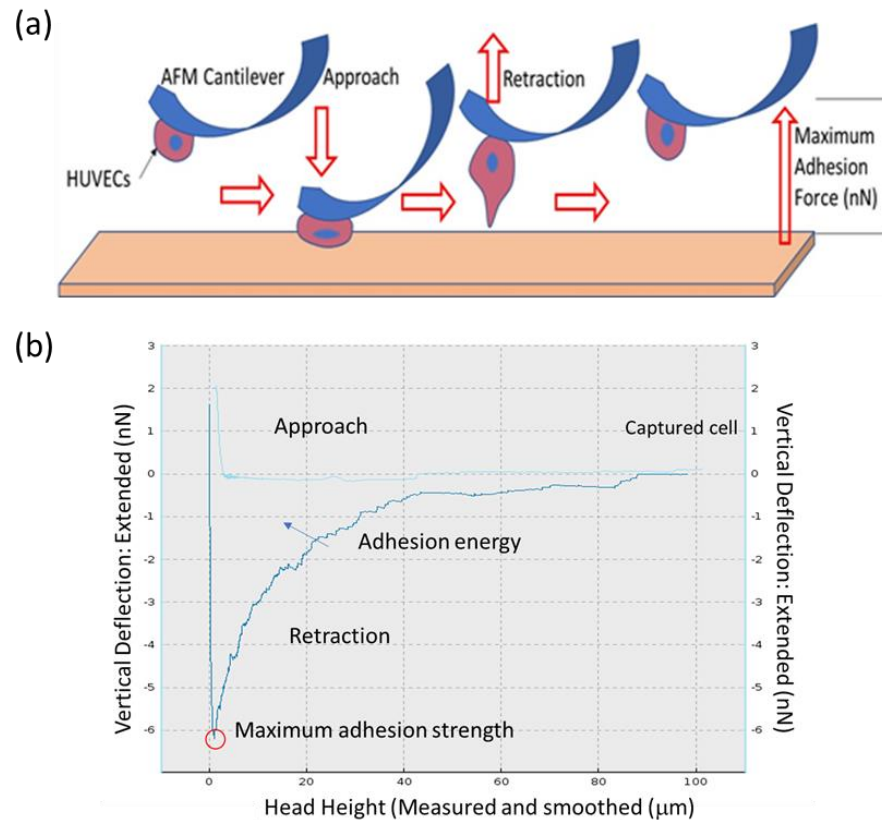


Figure 3. Schematic of (a) cell–substrate interaction measurement. (b) A force–distance (F-D) curve recorded with the CellHesion AFM technique.

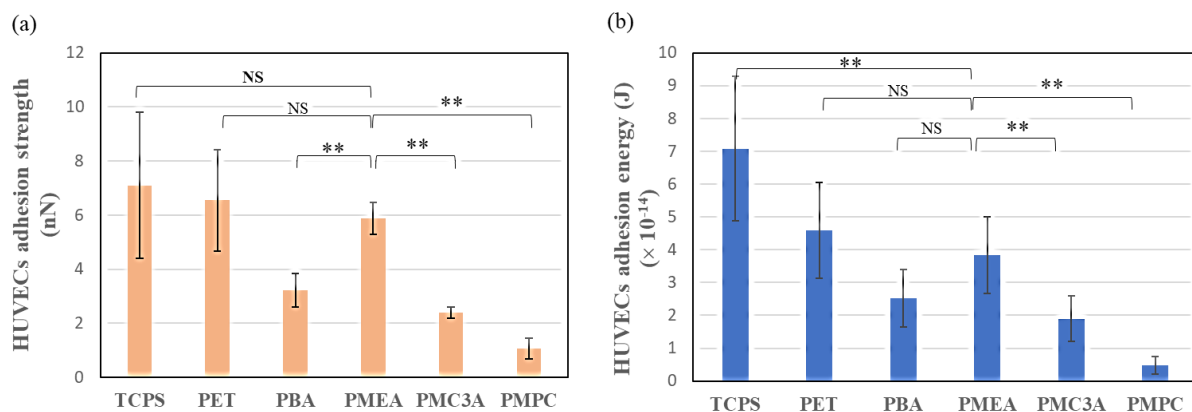


Figure 4. (a) HUVECs adhesion strength and (b) adhesion energy on various polymer substrates. The data represent the mean \pm SD ($n > 10$), ** $p < 0.05$ compared with PMEA and NS = Not Significant.

3.4. Human Platelet Adhesion Test

A platelet adhesion number test was performed under static conditions to evaluate the non-thrombogenic properties of PMEA-analogous polymers. The morphology and number of attached platelets were investigated using SEM. The result of the platelet adhesion test for each polymer-coated PET substrate is shown in Figure 5. Several platelets attached to the PET surface were also observed. A similar trend was observed for PBA-coated surfaces. In contrast, PMEA, PMC3A, and PMPC exhibited few platelet adhesions. Moreover, the

platelets attached to PMEa, PMC3A, and PMPC appeared mostly circular, unbranched, and distributed far away. The platelet area was also small, at approximately 2–5 μm . This implies that activation levels I to II, regularly I for PMPC and PMEa, were observed. In contrast, almost all of the attached platelets on PET and PBA exhibited activation levels of II to III. This implies that platelet spreading and proliferation occurred on the surface. The attached platelet area at approximately 5–10 μm had several branches.

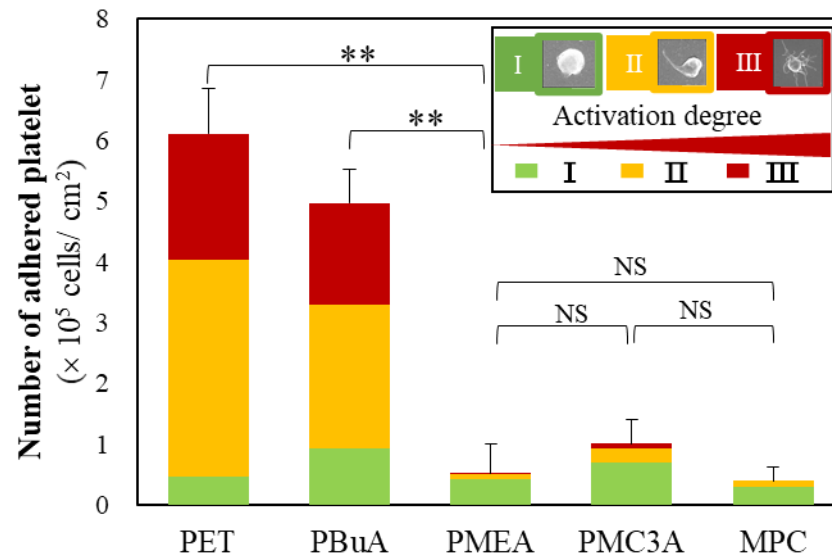


Figure 5. Summary of the human platelet adhesion experiments. Numbers of the adhered platelets on the coatings of the PMEa, PMC3A, PBA, PMPC, and bare PET. The data represent the means \pm SD, $n = 15$, **: $p < 0.01$ (vs. PET) and NS = Not Significant.

However, we still do not know how strongly or loosely the platelets adhered to the surface. As previously mentioned, shear stress affects adherent cells and platelet adhesion inside native blood vessels.

Furthermore, to investigate the platelet adhesion strength on PMEa-analogous polymers more quantitatively, we also used SCFS for platelets (Figure 6a). Similarly, platelet adhesion energy was calculated for each substrate. This adhesion energy represents the area under the retraction curve of the force curves obtained from the SCFS (Figure 6b). This reveals the total work conducted to detach platelets from their adherent state. A higher energy indicates a greater spread of platelets and strong adhesion to the substrates. We found that the adhesion force between platelets and PET had the highest interaction strength among all the polymers. The second highest level was platelet–PBA. Owing to the lack of IW in the chemical structures of PET and PBA, platelet adhesion protein adsorption increased. Therefore, platelets attached and denatured on these surfaces within a short time, and during retraction of the cantilever, more force was needed to detach the platelets from the surfaces. PMEa and PMC3A exhibited similar strengths, but lower strength compared to PET and PBA, whereas PMPC exhibited the lowest adhesion force. Moreover, the platelets were loosely attached to PMPC, PMEa, and PMC3A. These results also confirmed platelet adhesion on the test polymers under static conditions.

In addition, we have observed the oscillation in approach and retraction curve which is a little complicated to understand. According to the purpose, the same experimental condition was followed both for the platelet adhesion test at the static condition and for measuring the platelet adhesion strength. It can be clarified that the experiment was conducted using platelet-poor plasma (PPP) collected from whole human blood and single platelets. In PPP, the blood proteins density is still high and may create sublayers which influence the movement of the cantilever resulting in oscillation happening in the approach and retraction curve at 10 μm above the polymer interface. However, the practical interaction of platelet–polymer and detachment happened within 10 μm because of the small

size of a single platelet. Most of the measurements related to platelet adhesion force and adhesion energy showed similar tendencies.

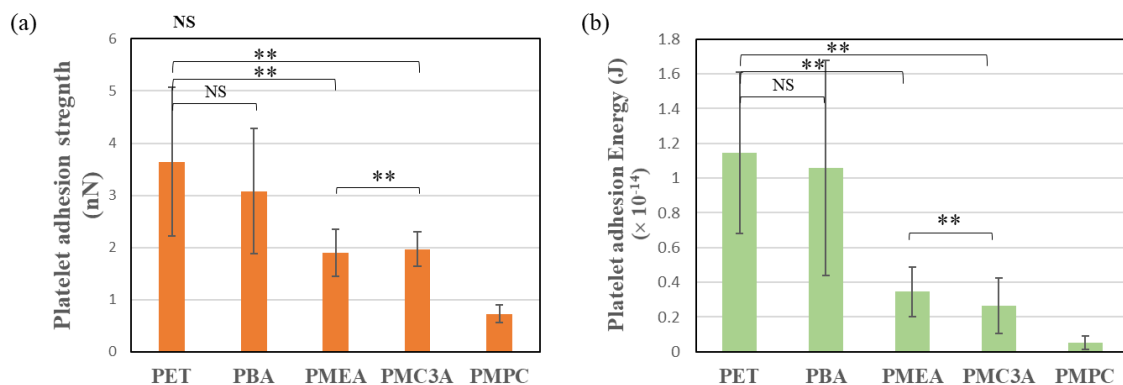


Figure 6. Comparison of (a) platelet adhesion strength and (b) adhesion energy on different polymer substrates. The data represent the mean \pm SD ($n > 5$), ** $p < 0.05$ (vs. PET and NS = Not Significant).

To determine the mechanism of platelet adhesion behavior, we previously reported that platelet adhesion is regulated by the amount of blood serum proteins or adhesion proteins that adhere to the polymer surface [8,38,41]. Fibrinogen and fibronectin are responsible for platelet adhesion. Fibrinogen is the plasma protein responsible for platelet adhesion [56], and it has been reported that the γ -chain of fibrinogen is related to the adhesion and activation of platelets, leading to thrombogenesis [56,57]. However, some synthetic polymers suppress platelet adhesion by suppressing fibrinogen adhesion [57]. The reason behind this property was attributed to the hydration layer formed at the interface. This hydration layer acts as a barrier between the serum protein and polymer surface. When synthetic polymers are exposed to the culture medium, PBS, or water, they adsorb water molecules at various positions in their chemical structures [8,47,58].

We initially indicated that Tanaka et al. reported that hydrated PMEA and its analogues contain IW. However, not all polymers are associated with these water molecules. All natural biopolymers were found to comprise IW on their surface, such as heparin, chondroitin sulfate, and DNA (RNA). Recently, it has been established that IW is a key factor in surface biocompatibility [42]. Sato et al. found different amounts of IW in hydrated PMEA analogues. They also reported that these hydrated PMEA analogues suppressed platelet adhesion by suppressing protein adsorption and deformation by increasing the amount of IW. Our platelet–substrate interaction study also demonstrated that the amount of IW might play a key role in expressing the blood compatibility of polymeric materials. If we order our polymer as IW content, we observed a similar tendency that platelet adhesion was suppressed as the IW increased, and the percentages of IW of the test polymers are listed in Table 1. Because PET and PBA do not contain any IW, serum proteins adhered to the surface. Consequently, the number of platelet adhesions was high. In contrast, PMPC, PMEA, and PMC3A exhibited low platelet counts on their surfaces. This is because IW exerts a repulsive effect against protein adsorption. Previously, we reported the spontaneous formation of numerous protrusions of the nanometer scale at the PMEA/phosphate-buffered saline (PBS) interfaces [47]. This result indicates the microphase separation of the polymer as polymer- and water-rich domains at the interfacial region [59]. Because of the partial imbroglia of the polymer chain in the bulk polymer phase, the mobility of the polymer chain is restricted at the interface, and phase separation occurs on the microscopic scale. The phase separation of a homopolymer at an interface is unique and makes an essential contribution to the blood compatibility of PMEA [60,61]. Our previous work also indicated that plasma protein fibrinogen exhibited adhesive interactions with the PMEA interface in polymer-rich domains, but repulsive interactions in water-rich domains [60]. In contrast, fibrinogen adhered to both the polymer- and water-rich domains on PBA, an analogous polymer of PMEA, exhibiting thrombogenic behavior. We considered that the differences

between PMEAs and PBAs were caused by differences in polymer density and hydration structures, particularly in the water-rich domains [57].

3.5. FM-AFM Observation of Coated Polymer Surfaces

FM-AFM is a powerful tool for investigating weak interactions on interfaces using the frequency shift associated with cantilever oscillation to detect interactions on a probe. In our previous work [62], we reported FM-AFM observations of polymer-grafted Au substrates of PMEAs, PMC3As, and PBAs, and that PMEAs and PMC3As exhibited a repulsive layer (mixed layer of polymer chains and hydration water) in water-rich domains. In contrast, PBA exhibited no repulsive layers in the water-rich domains. This difference may reflect the presence of IW on the interfaces. In this work, we performed FM-AFM to investigate the hydration states of spin-coated polymer films.

Figure 7a–e shows the results of FM-AFM (z - x scan) on each polymer/water interface, and Figure 7f shows the frequency shift (the intensity of the repulsion) as a function of distance from the interface obtained from the averaged cross section of the entire x -range. The repulsive layer is marked in blue and white, demonstrating the degree of frequency shift. The thickness of the repulsive layer on the PMPC was dramatically high at a thickness of approximately 20 nm. This thick hydration layer indicates a large amount of hydration at the PMPC/water interface and could be the reason for the extremely low HUVEC attachment and platelet adhesion. The thicknesses of the other polymers were relatively small; however, a clear trend was observed. The repulsive layer thickness decreased in the order of PMPC > PMEAs > PMC3A > PBA~PET. Interestingly, this trend is in accordance with the amount of hydrated water in the polymers (Table 1) and the trend of platelet adhesion (Figures 5 and 6). Therefore, we can expect that these repulsive layers on the spin-coated polymer films may originate from the mixed layer of polymer chains and hydration water on the interfaces, as well as our previous results obtained in the grafted polymer systems, and work to suppress platelet adhesion on the interfaces.

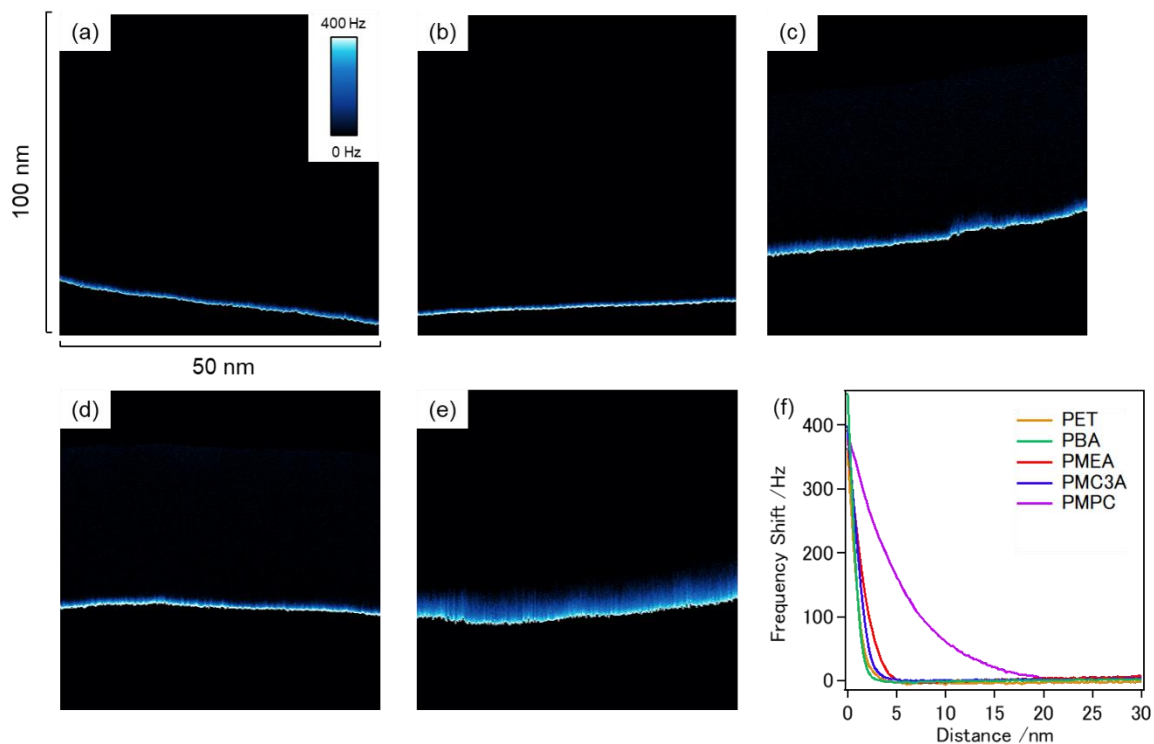


Figure 7. Images of FM-AFM z - x scan on (a) PET, (b) PBA, (c) PMEAs, (d) PMC3A, and (e) PMPC. (f) Frequency shift–distance curves obtained from the averaged cross section of (a–e).

3.6. Relationship between IW and Cell Adhesion Strength

Here we propose a possible explanation of the results observed in this study. We show the relationship between IW and cell adhesion strength in Figure 8. The HUVEC adhesion strength and number of adhered HUVECs and platelets on these substrates seem to be related to the IW content of each polymer. In this study, we investigated PME A-analogous polymers to find the most suitable polymer for use as a construction material for ASDBV development by the fulfilment of similar desired requirements of a native blood vessel. It is known that the native blood vessel has three layers: the adventitia or outer layer, which provides structural support and shape to the vessel; the tunica media, or a middle layer composed of elastic and muscular tissue that regulates the internal diameter of the vessel; and the tunic intima or an inner layer consisting of an endothelial lining that provides a frictionless pathway for blood movement [48]. Therefore, the surface of the artificial blood vessel should be biocompatible, non-thrombogenic, and have similar biochemical functions as native vessels.

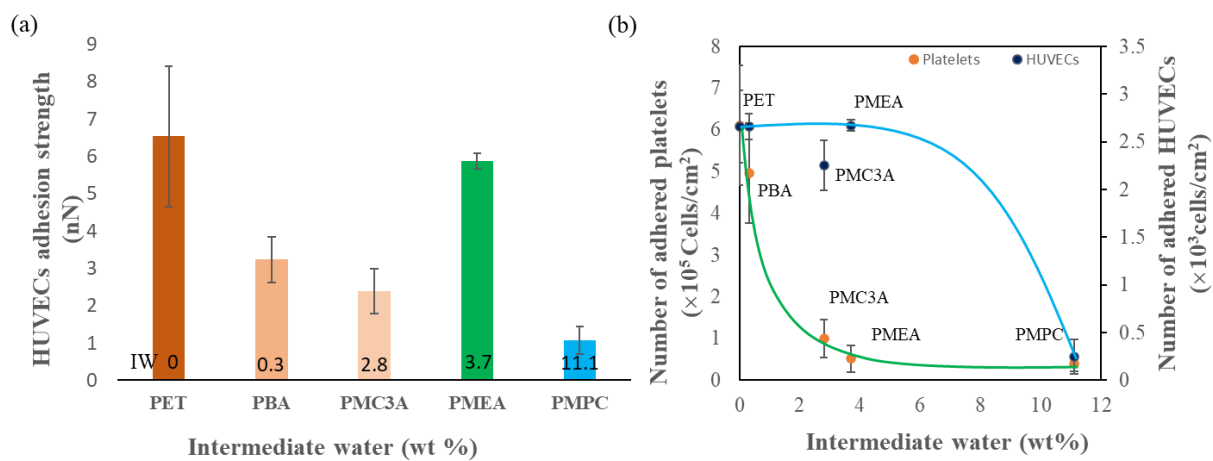


Figure 8. Effect of IW content on (a) HUVECs adhesion strength and (b) number of adhered platelets and HUVECs on PME A-analogous polymers.

First, we explicitly focused on the adhesion behavior of HUVECs on substrates. HUVECs attachment tests revealed how the number of attached cells decreased with increasing the IW, as shown in Figure 8b. From Figure 8b it seems there is a range, between 0 and 5 wt%, that did not influence the number of adhered cells. It would be attributable to the difference of the adsorption behavior between fibrinogen and fibronectin on the phase-separated surfaces as abovementioned. Similarly, HUVEC adhesion strength was more drastically enhanced on PME A than on PMC3A or PBA (Figure 8a). In addition, relationships between cell adhesion strength of cells (HUVECs and platelets) attached with substrates and contact angle measured by sessile drop, contact angle measured by captive air, hydration layer thickness, and bound water content (IW + NFW) are shown in Figure S5b in Supplementary Materials. From the above relation, all substrates showed good correlation with adhesion strength for platelets whereas relations for HUVECs adhesion strength were different. PME A did not follow the other analogues in terms of adhesion strength although it is a good sign for our purpose. We found the reasons that are related to the phase separation on the PME A hydrated surface due to IW content and protein adsorption behavior on those domains [49]. In addition, we compared platelet adhesion on the polymers. It was clear from both the normal adhesion test and platelet adhesion strength measurements that PME A and PMC3A effectively suppressed platelet adhesion, but PBA did not. These results indicate that PME A is an excellent candidate as a construction material for ASDBV development because it possesses both cytophilic and antithrombotic properties. In contrast, PMC3A suppressed both platelets and HUVEC, but PBA did not suppress either.

Additionally, the hydration state of the hydrated polymer surface was examined using FM-AFM for the first time. The thickness of the repulsive layer observed for each polymer agreed well with the trend of platelet adhesion and the amount of water in the polymers. As it is expected that the repulsive layer contains polymer chains and hydration water, the presence of the repulsive layer indicates the presence of water molecules interacting with the polymer chains on the interface, that is, IW. This result is consistent with our previous results demonstrating that IW suppresses fibrinogen adsorption and platelet adhesion at material interfaces. In the case of cell attachment, cells generally attach to the polymeric interface via cell-binding proteins. In serum-containing media, fibronectin, a cell adhesion protein, is responsible for cell adhesion through integrin, which is known as integrin-dependent cell adhesion [52]. Our recent work revealed that fibronectin easily interacts with the surface of biomaterials and causes conformational changes, even on PMEA. From the AFM observation of Nishida et al., polymer-rich domains show high hydrophobicity compared to polymer-poor (water-rich) domains [49]. In polymer-rich domains, fibrinogen adhesion force is similar to fibronectin, although conformational changes show small differences, with 42% for fibrinogen and 32% for fibronectin. In contrast, in polymer-poor regions, big differences were observed in both adhesion force and conformational changes, as fibronectin adhesion force was 0.34 nN, whereas it was 0.12nN for fibrinogen, and 72% conformational change occurred for fibronectin, whereas 24% change occurred for fibrinogen. Therefore, it can be said that cell adhesion and adhesion strength are regulated by fibronectin adsorption and conformational changes in polymer-poor domains which are composed of IW. The more fibronectin adsorption on polymer-poor domains, the more cells will be adhered through the integrin interaction which increases the focal interaction as well as adhesion strength. Furthermore, it has been reported that integrin-independent cell adhesion may occur on PMEA through direct interactions between the cell membrane and polymer surface [27]. This indicates that the difference in the trend of HUVEC attachment on PMEA, PMC3A, and PBA should be explained by other factors, not only the hydration layer on the interfaces. According to our purpose of study, the substrate should be consisting of both properties such as suppression of platelet adhesion and strong adhesion of endothelial cells. Only PMEA can exhibit these phenomena.

4. Conclusions

In conclusion, based on the conducted experiments, results, and discussion, the surface interactions of HUVECs were measured extensively. The IW content of PMEA-analogous polymers directly and indirectly influences the HUVEC adhesion strength and the number of adhered HUVECs and platelets on each substrate. It can be said that PMEA achieves the best outcomes among the analogues, such as low platelet adhesion and adhesion strength, high HUVECs attachment, proliferation, and high adhesion strength at the initial time. It can be suggested that PMEA can be used as a construction material to develop ASDBV because of its non-thrombogenic behavior and strong adhesion of endothelial cells. Finally, in this work, we examined the potential of PMEA for use in ASDBV at the initial stage, based on the interaction between the polymer interface and platelets and HUVEC. The cell behavior in the next stage, that is, monolayer formation of HUVEC on PMEA (HUVEC–HUVEC interaction) and the antithrombogenic property of the HUVEC monolayer (HUVEC–platelet interaction), will be reported in the next series of studies.

Supplementary Materials: The following supporting information can be downloaded from <https://www.mdpi.com/article/10.3390/surfaces5030027/s1>. Figure S1: Images of captured HUVEC, Figure S2: Images of captured platelet on cantilever during force with measurement by SCFS; Figure S3: Force curve of HUVEC–polymer, Figure S4: Force curve of platelet–polymer interaction, and Figure S5: Relationship between cell adhesion strength of HUVECs and platelets attached with substrates and contact angle, hydration layer thickness, and bound water content.

Author Contributions: Conceptualization: D.M. and M.T.; methodology: M.A.H., D.M. and M.T.; formal analysis: M.A.H.; investigation: M.A.H. and D.M.; data curation: M.A.H.; writing—original draft preparation: M.A.H.; writing—review and editing: D.M. and M.T.; supervision: D.M. and M.T.; project administration: M.T.; funding acquisition: M.T. All authors have read and agreed to the published version of the manuscript.

Funding: This study was funded by the Japan Society for the Promotion of Science (JSPS) (19H05720) from the Ministry of Education, Culture, Sports, Science, and Technology of Japan.

Institutional Review Board Statement: Not applicable.

Informed Consent Statement: Not applicable.

Data Availability Statement: The authors confirm that the data supporting the findings of this study are available within the article.

Acknowledgments: M.A.H. acknowledges the discussion with Kei Nishida and Tomoya Ueda. M.A.H. gratefully acknowledges the scholarship provided by the Ministry of Education, Culture, Sports, Science, and Technology (MEXT) of Japan. M.T. acknowledges the financial support from JSPS KAKENHI (grant number JP19H05720), the Funding Program for Next-Generation World-Leading Researchers (NEXT Program) of MEXT, and the Center of Innovation Program from the Japan Science and Technology Agency (JST). This work was partially supported by the Dynamic Alliance for Open Innovation Bridging of Human, Environment, and Materials.

Conflicts of Interest: The authors declare no conflict of interest.

References

1. Ratner, B.D.; Hoffman, A.S.; Schoen, F.J.; Lemons, J.E. Biomaterials science: An introduction to materials in medicine. *MRS Bull.* **2004**, *31*, 162–164.
2. Tsuruta, T. Contemporary Topics in Polymeric Materials for Biomedical Applications. *Adv. Polym. Sci.* **1996**, *126*, 1–55. [[CrossRef](#)]
3. Kim, S.H.; Turnbull, J.; Guimond, S. Extracellular matrix and cell signalling: The dynamic cooperation of integrin, proteoglycan and growth factor receptor. *J. Endocrinol.* **2011**, *209*, 139–151. [[CrossRef](#)] [[PubMed](#)]
4. Guilak, F.; Cohen, D.M.; Estes, B.T.; Gimble, J.M.; Liedtke, W.; Chen, C.S. Control of Stem Cell Fate by Physical Interactions with the Extracellular Matrix. *Cell Stem Cell.* **2009**, *5*, 17–26. [[CrossRef](#)]
5. Giancotti, F.G.; Ruoslahti, E. Integrin signaling. *Science* **1999**, *285*, 1028–1033. [[CrossRef](#)]
6. Anselme, K.; Biggerelle, M. Modelling approach in cell/material interactions studies. *Biomaterials* **2006**, *27*, 1187–1199. [[CrossRef](#)] [[PubMed](#)]
7. Harburger, D.S.; Calderwood, D.A. Integrin signalling at a glance. *J. Cell Sci.* **2009**, *122*, 159–163. [[CrossRef](#)]
8. Tanaka, M.; Motomura, T.; Kawada, M.; Anzai, T.; Kasori, Y.; Shiroya, T.; Shimura, K.; Onishi, M.; Mochizuki, A. Blood compatible aspects of poly(2-methoxyethylacrylate) (PMEA)-relationship between protein adsorption and platelet adhesion on PMEA surface. *Biomaterials* **2000**, *21*, 1471–1481. [[CrossRef](#)]
9. Radke, D.; Jia, W.; Sharma, D.; Fena, K.; Wang, G.; Goldman, J.; Zhao, F. Tissue Engineering at the Blood-Contacting Surface: A Review of Challenges and Strategies in Vascular Graft Development. *Adv. Healthc. Mater.* **2018**, *7*, e1701461. [[CrossRef](#)]
10. Marchio, P.; Guerra-Ojeda, S.; Vila, J.M.; Aldasoro, M.; Victor, V.M.; Mauricio, M.D. Targeting early atherosclerosis: A focus on oxidative stress and inflammation. *Oxidative Med. Cell. Longev.* **2019**, *2019*, 8563845. [[CrossRef](#)]
11. Libby, P.; Buring, J.E.; Badimon, L.; Hansson, G.K.; Deanfield, J.; Bittencourt, M.S.; Tokgözoğlu, L.; Lewis, E.F. Atherosclerosis. *Nat. Rev. Dis. Primers* **2019**, *5*, 56. [[CrossRef](#)] [[PubMed](#)]
12. Mallis, P.; Kostakis, A.; Stavropoulos-Giokas, C.; Michalopoulos, E. Future perspectives in small-diameter vascular graft engineering. *Bioengineering* **2020**, *7*, 160. [[CrossRef](#)] [[PubMed](#)]
13. Xue, L.; Greisler, H.P. Biomaterials in the development and future of vascular grafts. *J. Vasc. Surg.* **2003**, *37*, 472–480. [[CrossRef](#)]
14. Fang, J.; Li, S. Advances in vascular tissue engineering. *J. Med. Biomech.* **2016**, *31*, E333–E339. [[CrossRef](#)]
15. Tara, S.; Rocco, K.A.; Hibino, N.; Sugiura, T.; Kurobe, H.; Breuer, C.K.; Shinoka, T. Vessel Bioengineering. *Circ. J.* **2014**, *78*, 12–19. [[CrossRef](#)] [[PubMed](#)]
16. Gao, A.; Hang, R.; Li, W.; Zhang, W.; Li, P.; Wang, G.; Bai, L.; Yu, X.F.; Wang, H.; Tong, L.; et al. Linker-free covalent immobilization of heparin, SDF-1 α , and CD47 on PTFE surface for antithrombogenicity, endothelialization and anti-inflammation. *Biomaterials* **2017**, *140*, 201–211. [[CrossRef](#)] [[PubMed](#)]
17. Weidenbacher, L.; Müller, E.; Guex, A.G.; Zündel, M.; Schweizer, P.; Marina, V.; Adlhart, C.; Vejsadová, L.; Pauer, R.; Spiecker, E.; et al. In Vitro Endothelialization of Surface-Integrated Nanofiber Networks for Stretchable Blood Interfaces. *ACS Appl. Mater. Interfaces* **2019**, *11*, 5740–5751. [[CrossRef](#)]
18. Noy, J.-M.; Chen, F.; Akhter, D.T.; Houston, Z.H.; Fletcher, N.L.; Thurecht, K.J.; Stenzel, M.H. Direct Comparison of Poly(ethylene glycol) and Phosphorylcholine Drug-Loaded Nanoparticles In Vitro and In Vivo. *Biomacromolecules* **2020**, *21*, 2320–2333. [[CrossRef](#)]

19. Furuzono, T.; Ishihara, K.; Nakabayashi, N.; Tamada, Y. Chemical modification of silk fibroin with 2-methacryloyloxyethyl phosphorylcholine. II. Graft-polymerization onto fabric through 2-methacryloyloxyethyl isocyanate and interaction between fabric and platelets. *Biomaterials* **2000**, *21*, 327–333. [[CrossRef](#)]
20. Park, H.H.; Sun, K.; Seong, M.; Kang, M.; Park, S.; Hong, S.; Jung, H.; Jang, J.; Kim, J.; Jeong, H.E. Lipid-Hydrogel-Nanostructure Hybrids as Robust Biofilm-Resistant Polymeric Materials. *ACS Macro Lett.* **2019**, *8*, 64–69. [[CrossRef](#)]
21. Suhara, H.; Sawa, Y.; Nishimura, M.; Oshiyama, H.; Yokoyama, K.; Saito, N.; Matsuda, H. Efficacy of a new coating material, PMEA, for cardiopulmonary bypass circuits in a porcine model. *Ann. Thorac. Surg.* **2001**, *71*, 1603–1608. [[CrossRef](#)]
22. Hatakeyama, H.; Hatakeyama, T. Interaction between water and hydrophilic polymers. *Thermochim. Acta* **1998**, *308*, 3–22. [[CrossRef](#)]
23. Morita, S.; Tanaka, M.; Ozaki, Y. Time-resolved in situ ATR-IR observations of the process of sorption of water into a poly(2-methoxyethyl acrylate) film. *Langmuir* **2007**, *23*, 3750–3761. [[CrossRef](#)]
24. Miwa, Y.; Ishida, H.; Saitô, H.; Tanaka, M.; Mochizuki, A. Network structures and dynamics of dry and swollen poly(acrylate)s. Characterization of high- and low-frequency motions as revealed by suppressed or recovered intensities (SRI) analysis of ¹³C NMR. *Polymer* **2009**, *50*, 6091–6099. [[CrossRef](#)]
25. Tanaka, M.; Motomura, T.; Ishii, N.; Shimura, K.; Onishi, M.; Mochizuki, A.; Hatakeyama, T. Cold crystallization of water in hydrated poly(2-methoxyethyl acrylate) (PMEA). *Polym. Int.* **2000**, *49*, 1709–1713. [[CrossRef](#)]
26. Hoshihara, T.; Nikaido, M.; Tanaka, M. Characterization of the attachment mechanisms of tissue-derived cell lines to blood-compatible polymers. *Adv. Healthc. Mater.* **2014**, *3*, 775–784. [[CrossRef](#)] [[PubMed](#)]
27. Hoshihara, T.; Yoshihiro, A.; Tanaka, M. Evaluation of initial cell adhesion on poly (2-methoxyethyl acrylate) (PMEA) analogous polymers. *J. Biomater. Sci. Polym. Ed.* **2017**, *28*, 986–999. [[CrossRef](#)] [[PubMed](#)]
28. Medina-Leyte, D.J.; Domínguez-Pérez, M.; Mercado, I.; Villarreal-Molina, M.T.; Jacobo-Albavera, L. Use of human umbilical vein endothelial cells (HUVEC) as a model to study cardiovascular disease: A review. *Appl. Sci.* **2020**, *10*, 938. [[CrossRef](#)]
29. Baudin, B.; Bruneel, A.; Bosselut, N.; Vaubourdoles, M. A protocol for isolation and culture of human umbilical vein endothelial cells. *Nat. Protoc.* **2007**, *2*, 481–485. [[CrossRef](#)]
30. Onat, D.; Brillion, D.; Colombo, P.C.; Schmidt, A.M. Human vascular endothelial cells: A model system for studying vascular inflammation in diabetes and atherosclerosis. *Curr. Diabetes Rep.* **2011**, *11*, 193–202. [[CrossRef](#)]
31. Schleger, C.; Platz, S.J.; Deschl, U. Development of an in vitro model for vascular injury with human endothelial cells. *ALTEX Altern. Anim. Exp.* **2004**, *21*, 12–19.
32. Vion, A.C.; Ramkhalawon, B.; Loyer, X.; Chironi, G.; Devue, C.; Loirand, G.; Tedgui, A.; Lehoux, S.; Boulanger, C.M. Shear stress regulates endothelial microparticle release. *Circ. Res.* **2013**, *112*, 1323–1333. [[CrossRef](#)] [[PubMed](#)]
33. Fearon, I.M.; Gaça, M.D.; Nordskog, B.K. In vitro models for assessing the potential cardiovascular disease risk associated with cigarette smoking. *Toxicol. In Vitro* **2013**, *27*, 513–522. [[CrossRef](#)] [[PubMed](#)]
34. Sato, C.; Aoki, M.; Tanaka, M. Blood-compatible poly(2-methoxyethyl acrylate) for the adhesion and proliferation of endothelial and smooth muscle cells. *Colloids Surf. B Biointerfaces* **2016**, *145*, 586–596. [[CrossRef](#)]
35. Asai, F.; Seki, T.; Hoshino, T.; Liang, X.; Nakajima, K.; Takeoka, Y. Silica Nanoparticle Reinforced Composites as Transparent Elastomeric Damping Materials. *ACS Appl. Nano Mater.* **2021**, *4*, 4140–4152. [[CrossRef](#)]
36. Asai, F.; Seki, T.; Sugawara-Narutaki, A.; Sato, K.; Odent, J.; Coulembier, O.; Raquez, J.M.; Takeoka, Y. Tough and Three-Dimensional-Printable Poly(2-methoxyethyl acrylate)-Silica Composite Elastomer with Antiplatelet Adhesion Property. *ACS Appl. Mater. Interfaces* **2020**, *12*, 46621–46628. [[CrossRef](#)]
37. Watanabe, K.; Miwa, E.; Asai, F.; Seki, T.; Urayama, K.; Nakatani, T.; Fujinami, S.; Hoshino, T.; Takata, M.; Liu, C.; et al. Highly Transparent and Tough Filler Composite Elastomer Inspired by the Cornea. *ACS Mater. Lett.* **2020**, *2*, 325–330. [[CrossRef](#)]
38. Kobayashi, S.; Wakui, M.; Iwata, Y.; Tanaka, M. Poly(ω -methoxyalkyl acrylate)s: Nonthrombogenic Polymer Family with Tunable Protein Adsorption. *Biomacromolecules* **2017**, *18*, 4214–4223. [[CrossRef](#)]
39. Nishida, K.; Anada, T.; Kobayashi, S.; Ueda, T.; Tanaka, M. Effect of bound water content on cell adhesion strength to water-insoluble polymers. *Acta Biomater.* **2021**, *134*, 313–324. [[CrossRef](#)]
40. Friedrichs, J.; Legate, K.R.; Schubert, R.; Bharadwaj, M.; Werner, C.; Müller, D.J.; Benoit, M. A practical guide to quantify cell adhesion using single-cell force spectroscopy. *Methods* **2013**, *60*, 169–178. [[CrossRef](#)]
41. Sato, K.; Kobayashi, S.; Kusakari, M.; Watahiki, S.; Oikawa, M.; Hoshihara, T.; Tanaka, M. The Relationship between Water Structure and Blood Compatibility in Poly(2-methoxyethyl Acrylate) (PMEA) Analogues. *Macromol. Biosci.* **2015**, *15*, 1296–1303. [[CrossRef](#)] [[PubMed](#)]
42. Tanaka, M.; Kobayashi, S.; Murakami, D.; Aratsu, F.; Kashiwazaki, A.; Hoshihara, T.; Fukushima, K. Design of Polymeric Biomaterials: The “Intermediate Water Concept”. *Bull. Chem. Soc. Jpn.* **2019**, *92*, 2043–2057. [[CrossRef](#)]
43. Morita, S.; Tanaka, M.; Kitagawa, K.; Ozaki, Y. Hydration structure of poly(2-methoxyethyl acrylate): Comparison with a 2-methoxyethyl acetate model monomer. *J. Biomater. Sci. Polym. Ed.* **2010**, *21*, 1925–1935. [[CrossRef](#)] [[PubMed](#)]
44. Kuo, A.T.; Sonoda, T.; Urata, S.; Koguchi, R.; Kobayashi, S.; Tanaka, M. Elucidating the Feature of Intermediate Water in Hydrated Poly(ω -methoxyalkyl acrylate)s by Molecular Dynamics Simulation and Differential Scanning Calorimetry Measurement. *ACS Biomater. Sci. Eng.* **2020**, *6*, 3915–3924. [[CrossRef](#)] [[PubMed](#)]
45. Hancock, B.C.; Zografi, G. The Relationship Between the Glass Transition Temperature and the Water Content of Amorphous Pharmaceutical Solids. *Pharm. Res.* **1994**, *11*, 471–477. [[CrossRef](#)]

46. Hoshiba, T.; Orui, T.; Endo, C.; Sato, K.; Yoshihiro, A.; Minagawa, Y.; Tanaka, M. Adhesion-based simple capture and recovery of circulating tumor cells using a blood-compatible and thermo-responsive polymer-coated substrate. *RSC Adv.* **2016**, *6*, 89103–89112. [[CrossRef](#)]
47. Murakami, D.; Kobayashi, S.; Tanaka, M. Interfacial Structures and Fibrinogen Adsorption at Blood-Compatible Polymer/Water Interfaces. *ACS Biomater. Sci. Eng.* **2016**, *2*, 2122–2126. [[CrossRef](#)]
48. Tucker, W.D.; Arora, Y.; Mahajan, K. *Anatomy, Blood Vessels*; StatPearls: Treasure Island, FL, USA, 2021.
49. Nishida, K.; Baba, K.; Murakami, D.; Tanaka, M. Nanoscopic analyses of cell-adhesive protein adsorption on poly(2-methoxyethyl acrylate) surfaces. *Biomater. Sci.* **2022**, *10*, 2953–2963. [[CrossRef](#)]
50. Mescola, A.; Canale, C.; Prato, M.; Diaspro, A.; Berdondini, L.; Maccione, A.; Dante, S. Specific Neuron Placement on Gold and Silicon Nitride-Patterned Substrates through a Two-Step Functionalization Method. *Langmuir* **2016**, *32*, 6319–6327. [[CrossRef](#)]
51. Oropesa-Nuñez, R.; Mescola, A.; Vassalli, M.; Canale, C. Impact of experimental parameters on cell–cell force spectroscopy signature. *Sensors* **2021**, *21*, 1069. [[CrossRef](#)]
52. Hozumi, K.; Otagiri, D.; Yamada, Y.; Sasaki, A.; Fujimori, C.; Wakai, Y.; Uchida, T.; Katagiri, F.; Kikkawa, Y.; Nomizu, M. Cell surface receptor-specific scaffold requirements for adhesion to laminin-derived peptide-chitosan membranes. *Biomaterials* **2010**, *31*, 3237–3243. [[CrossRef](#)] [[PubMed](#)]
53. Hersel, U.; Dahmen, C.; Kessler, H. RGD modified polymers: Biomaterials for stimulated cell adhesion and beyond. *Biomaterials* **2003**, *24*, 4385–4415. [[CrossRef](#)]
54. Tersteeg, C.; Roest, M.; Mak-Nienhuis, E.M.; Ligtenberg, E.; Hofer, I.E.; de Groot, P.G.; Pasterkamp, G. A fibronectin-fibrinogen-tropoelastin coating reduces smooth muscle cell growth but improves endothelial cell function. *J. Cell. Mol. Med.* **2012**, *16*, 2117–2126. [[CrossRef](#)] [[PubMed](#)]
55. Dejana, E.; Colella, S.; Languino, L.R.; Balconi, G.; Corbascio, G.C.; Marchisio, P.C. Fibrinogen induces adhesion, spreading, and microfilament organization of human endothelial cells in vitro. *J. Cell Biol.* **1987**, *104*, 1403–1411. [[CrossRef](#)] [[PubMed](#)]
56. Tsai, W.B.; Grunkemeier, J.M.; Horbett, T.A. Human plasma fibrinogen adsorption and platelet adhesion to polystyrene. *J. Biomed. Mater. Res.* **1999**, *44*, 130–139. [[CrossRef](#)]
57. Murakami, D.; Segami, Y.; Ueda, T.; Tanaka, M. Control of interfacial structures and anti-platelet adhesion property of blood-compatible random copolymers. *J. Biomater. Sci. Polym. Ed.* **2020**, *31*, 207–218. [[CrossRef](#)]
58. Tanaka, M.; Mochizuki, A.; Ishii, N.; Motomura, T.; Hatakeyama, T. Study of blood compatibility with poly(2-methoxyethyl acrylate). Relationship between water structure and platelet compatibility in poly(2-methoxyethylacrylate-co-2-hydroxyethylmethacrylate). *Biomacromolecules* **2002**, *3*, 36–41. [[CrossRef](#)]
59. Murakami, D.; Kitahara, Y.; Kobayashi, S.; Tanaka, M. Thermosensitive Polymer Biocompatibility Based on Interfacial Structure at Biointerface. *ACS Biomater. Sci. Eng.* **2018**, *4*, 1591–1597. [[CrossRef](#)]
60. Ueda, T.; Murakami, D.; Tanaka, M. Analysis of interaction between interfacial structure and fibrinogen at blood-compatible polymer/water interface. *Front. Chem.* **2018**, *6*, 542. [[CrossRef](#)]
61. Murakami, D.; Mawatari, N.; Sonoda, T.; Kashiwazaki, A.; Tanaka, M. Effect of the Molecular Weight of Poly(2-methoxyethyl acrylate) on Interfacial Structure and Blood Compatibility. *Langmuir* **2019**, *35*, 2808–2813. [[CrossRef](#)]
62. Murakami, D.; Nishimura, S.n.; Tanaka, Y.; Tanaka, M. Observing the repulsion layers on blood-compatible polymer-grafted interfaces by frequency modulation atomic force microscopy. *Mater. Sci. Eng. C* **2021**, *133*, 112596. [[CrossRef](#)] [[PubMed](#)]